An Interpenetrated System Based on a Tetrafunctional Epoxy Resin and a Thermosetting Bismaleimide: Structure–Properties Correlation

PELLEGRINO MUSTO, EZIO MARTUSCELLI, GIUSEPPE RAGOSTA, PIETRO RUSSO, GENNARO SCARINZI

National Research Council of Italy, Institute of Research and Technology of Plastic Materials, Via Toiano no. 6, 80072 Arco Felice (NA), Italy

Received 2 May 1997; accepted 26 August 1997

ABSTRACT: The kinetics and mechanism of the curing process of a thermosetting blend formed by tetraglycidyl-4,4′-diaminodiphenyl methane and *N*,*N*′-bismaleimido-4,4′-diphenyl methane (BMI) cured in the presence of 4,4′-diaminodiphenyl sulfone, was investigated in detail by Fourier transform infrared spectroscopy. Information on the molecular structure of the network formed upon curing was derived. Dynamic-mechanical measurements on dry samples indicated an interpenetrated polymer network-like structure. Sorption measurements at 70°C showed a reduction of the water uptake at equilibrium in the presence of substantial amounts of BMI in the system (43.5% body weight). Finally, the dynamic-mechanical analysis of wet samples demonstrated a reduction of the plasticizing efficiency of the absorbed water in the presence of BMI.
 J Appl Polym Sci 69: 1029–1042, 1998

Key words: epoxy resins; bismaleimides; FTIR spectroscopy; interpenetrating polymer networks (IPNs); curing kinetics

INTRODUCTION

Epoxy resins are one of the most important classes of thermosetting matrices for composite applications. In particular, the tetraglycidyl-4,4′-diaminodiphenyl methane (TGDDM) cured by aromatic diamines [such as diaminodiphenyl sulfone (DDS)] is widely used as matrix material in carbon fiber-reinforced structural composites in the aircraft and aerospace industries. However, the TGDDM/DDS system suffers from two main limitations: the brittleness and the high levels of moisture absorption that adversely affect its mechanical performances. With respect to the first problem, modification of the base resin with either thermoplastics[1–3] or conventional liquid rubbers[4,5] has been reported. To overcome the second limitation, a promising approach has recently emerged, which consists in the formulation of thermoset/thermoset blends. These systems generally belong to the class of intercrosslinked or interpenetrated polymer networks (IPNs). Owing to their peculiar molecular structure, these complex networks often exhibit synergistic effects, which produce considerable and unexpected improvements in some properties with respect to those of the neat components.[6]

In this article, we report on a blend system in which the TGDDM/DDS resin is mixed with a bismaleimide [*N*,*N*′-bismaleimide-4,4′-diphenyl methane (BMI)] monomer. The BMI exhibits a superior chain rigidity than the epoxy, and hence

Correspondence to: P. Musto.

Journal of Applied Polymer Science, Vol. 69, 1029–1042 (1998)
 CCC 0021-8995/98/051029-14

higher values of T_g when fully cured, excellent thermal and thermo-oxidative stability, and a negligible tendency to absorb water. On the other hand, the BMI resin is a crystalline powder very difficult to process, because thermal curing starts at temperatures just above the melting point. In principle, a suitably formulated blend should exhibit a tendency to absorb atmospheric moisture much lower than that of the TGDDM matrix and a much better processability than that of the BMI resin.

The kinetics of the complex curing process of this system has been investigated in detail, for a typical composition, by Fourier transform infrared (FTIR) spectroscopy. The results allowed an insight in the reaction mechanism as well as in the network's molecular structure that develops upon curing. Specimens with different amounts of BMI were prepared and characterized with respect to their dynamic-mechanical behavior, mechanical properties, and water sorption. It is shown that the presence of BMI improves such properties as the T_g and stiffness, while reducing the water uptake of the resin.

EXPERIMENTAL

Materials

The epoxy resin was a commercial grade TGDDM supplied by Ciba Geigy (Basel, Switzerland) and was cured by DDS from Aldrich (Milwaukee, WI). BMI was also from Aldrich. The chemical formulas of the system components are reported herein.

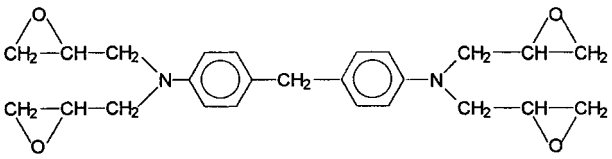

TGDDM: Tetraglycidyl epoxide based on DDM

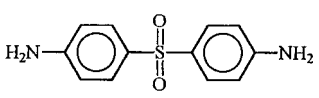

DDS: 4, 4' diamino dipheny sulfone

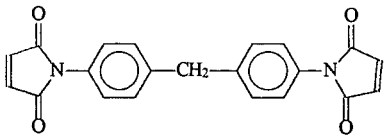

BMI: N, N' bismaleimido-4, 4'-diphenyl methane

Preparation of a Typical TGDDM/DDS/BMI Blend

Thirty phr of DDS were dissolved into the TGDDM resin at 120°C under vigorous mechanical stirring. After complete dissolution, the mixture was degassed under vacuum and the appropriate amount of BMI was added. Mixing was continued at 100°C until a clear and visually homogeneous mixture was obtained. The reactive mixture was then poured in a glass mold, cured at 140°C for 16 h, and postcured for 4 h at 200°C.

The compositions of the investigated mixtures are reported in Table I.

Techniques

FTIR spectra were collected on thin films (5–15 μm) of the reactive mixture, obtained by casting 10% wt/wt acetone solutions onto KBr disks. Most of the solvent was allowed to evaporate at room temperature, and final drying of the samples was conducted in a vacuum oven at 70°C for 1 h. No traces of residual solvent were detectable spectroscopically in the samples. The film thickness was chosen to keep the peaks of interest in an absorbance range where the Lambert–Beer law is verified (up to 1.2 absorbance units).

Spectra were obtained at a resolution of 2 cm^{-1} using a Perkin–Elmer System 2000 spectrometer. The instrument was equipped with a deuterated triglycine sulfate detector and a Ge/KBr beam splitter. The scanned wavenumber range was 4000–400 cm^{-1}. The isothermal kinetic measurements were performed in a SPECAC 80100 environmental chamber directly mounted in the spectrometer and purged continuously with dry nitrogen. This unit was controlled by an Eurotherm 071 temperature controller to an accuracy of ±1°C.

Dynamic-mechanical measurements at 1 Hz were made in the single-cantilever bending mode using a Polymer Laboratories (UK) dynamic mechanical thermal analyzer apparatus.

The elastic modulus, E, was measured in flexural mode using an Instron mechanical tester at

Table I Compositions of the Investigated Blends

TGDDM (parts/ body wt.)	DDS (parts/ body wt.)	BMI (parts/ body wt.)	TGDDM (wt %)	DDS (wt %)	BMI (wt %)	Epoxy Groups[a] (mol kg^{-1})	Amino Groups (mol kg^{-1})	BMI Double Bonds (mol kg^{-1})
100	30	—	76.9	23.1	—	6.19	3.69	—
100	30	10	71.4	21.5	7.1	5.75	3.43	0.40
100	30	30	62.6	18.7	18.7	5.03	3.00	1.05
100	30	50	55.5	16.6	27.9	4.47	2.66	1.55
100	30	100	43.5	13.0	43.5	2.08	0.56	2.43

[a] By potentiometric titration.

ambient temperature and at a crosshead speed of 1 mm min^{-1}.

Three-point bending specimens 60.0 mm long, 6.0 mm wide, and 4.0 mm thick were used to perform fracture tests using the same apparatus and the same testing conditions as described. Before testing, the samples were sharply notched. Fracture data were analyzed according to the concepts of linear elastic fracture mechanics.[7]

The critical stress intensity factor, K_c, was calculated by means of the equation:

$$K_c = Y\sigma\sqrt{a} \quad (1)$$

where σ is the nominal stress at the onset of crack propagation, a is the initial crack length, and Y is a calibration factor depending on the specimen geometry. For three-point bending specimens, Y is given by Brown and Srawley.[8] For the determination of the critical strain energy release rate, G_c, the following equation was used:

$$G_c = U/BW\phi \quad (2)$$

where U is the fracture energy; B and W are the thickness and the width of the specimen, respectively; and ϕ is a calibration factor that depends on the length of the notch and size of the sample. Values of ϕ were taken from Plati and Williams.[9]

RESULTS AND DISCUSSION

Curing Kinetics and Molecular Structure

The FTIR spectra of a neat TGDDM/DDS resin and of a 100/30/100 parts per body weight TGDDM/DDS/BMI mixture, before the curing process, are shown in Figs. 1(a,b;) curves A and B, respectively). In particular, Fig. 1(a) displays the 4000–2500 cm^{-1} spectral range, whereas Fig. 1(b) reports the 2000–500 cm^{-1} interval. In the same figures, curve C displays a difference spectrum obtained by subtracting the spectrum of the neat resin from that of the TGDDM/DDS/BMI mixture. The subtraction factor was estimated by reducing to the baseline the TGDDM/DDS doublet at 1614–1594 cm^{-1}. The result is representative of the spectrum of the BMI within the reactive mixture and, in the whole frequency range, appears very "clean." A first derivative-type feature, indicative of peak shift between the sample and the reference spectra, is detected only at about 3380 cm^{-1}. This frequency corresponds to the intense symmetric stretching mode of the primary amine group and a shift toward higher wavenumbers in the presence of BMI might indicate a perturbation of the hydrogen bonding interactions involving these groups. The peak at 3472 cm^{-1}, which corresponds to the frequency of the asymmetric stretching mode of the primary amine, is not due to incomplete subtraction but to the first overtone absorption of the imide carbonyl stretching at 1714 cm^{-1}. The rest of the spectrum corresponds very closely to that of BMI dissolved in a low polarity solvent (i.e., CH_2Cl_2). In particular, the characteristic crystal field splitting of most of the peaks that is readily observed in the BMI powder spectrum is completely absent. This provides clear evidence that the BMI is completely dissolved (i.e., at molecular level) in the TGDDM/DDS mixture and that no microcrystalline structures are present in the system before the curing process. The most relevant BMI absorptions for the subsequent kinetic analysis are those occurring at 3472, 3097, and 827 cm^{-1}. The first, as already noted, is a $\nu_{C=O}$ overtone and interferes

with the ν_{as} of the NH_2 group that is used to evaluate the primary amine concentration in the system. However, its absolute intensity is invariant during curing, and appropriate correction of the analytical band intensity is therefore possible. The peak at 3097 is due to the ν(H—C=) vibration and has been widely used in the literature[10,11] to follow the conversion of BMI double bonds during curing. In the system under investigation, it is poorly resolved from the complex profile due to the C—H stretching modes at lower frequency. Finally, the sharp and medium intensity peak at 827 cm^{-1} has been variously interpreted in the literature. Recently, however, vibrational analysis of plane and deuterated model compounds[12] allowed unambiguous assignment of this absorption to an out-of-plane bending of the H—C= unit, thus allowing such a peak to be successfully used in polymerization kinetics investigations.[3,13]

A kinetic analysis was performed at 140°C, which is the curing temperature (see the Experimental section), to obtain information on the reaction mechanism and on the molecular structure of this complex network, as developed upon curing.

In principle, in a TGDDM/DDS/BMI system, several chemical reactions may occur, either simultaneously or at different stages of the curing process, depending on the relative reactivity of the components and on the process temperature. As far as the epoxy/hardener pair is concerned, there are three main reactions that may take place[14]:

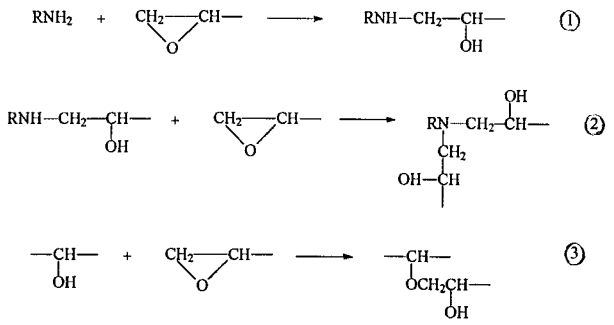

Steps 1 and 2 are the primary and secondary amine reactions with the glycidyl ether, and step 3 is an etherification reaction of the glycidyl ether by a pendant hydroxyl group. Reactions 1 and 2 are also catalyzed by the presence of hydroxyl groups that are created by the amine reactions themselves (which accounts for the autocatalytic nature of the process) and sometimes added in the formulation as an accelerator. The reactivities of the primary and secondary amino groups may be different, with the former being higher, but no general consensus exists in the literature on the value of the ratio between the rate constants of these two steps.[14] This ratio is indeed supposed to have a strong effect on the cure process. The tendency of the etherification reaction (step 3) to occur depends on the temperature, on the basicity of the amine, and on the composition of the reactive mixture.

In the presence of aromatic amines, the bismaleimides may undergo two different reactions, which are shown below:

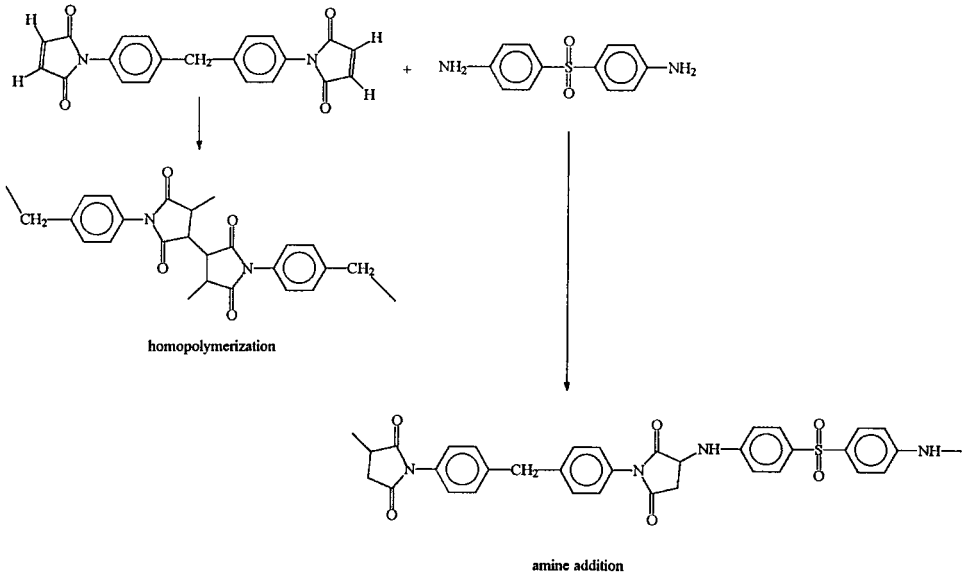

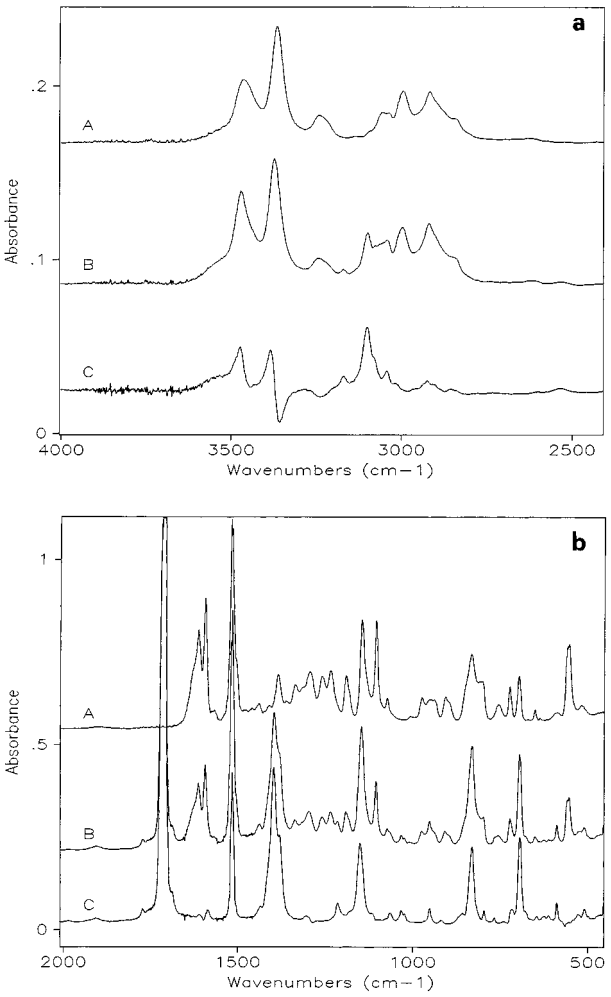

Figure 1 Transmission FTIR spectra of the neat epoxy resin (curve A), of the TGDDM/DDS/BMI system (curve B), and the subtraction spectrum B − A (curve C). (a) Frequency range of 4000–2500 cm^{-1}. (b) Relative to the 2000–500 cm^{-1} interval.

As a matter of fact, the bismaleimides are generally cross-linked *via* a two-step process in which chain extension by Michael addition and radical homopolymerization take place either sequentially or simultaneously depending on the curing temperature. Michael addition has the effect of reducing the crosslinking density of the resin, thus improving its flexibility. The vast majority of the authors agree[15–18] that the Michael addition is faster and occurs at lower temperatures than the homopolymerization reaction; although, in a recent contribution, Lin and Chen[19]—based on calorimetric data—drew the opposite conclusion.

In the system under investigation, the hardener (DDS) is common to both the thermosetting resins. If the amine reacts simultaneously with TGDDM and BMI, an intercrosslinked network will be formed in which the network chains are constituted by a TGDDM/DDS/BMI copolymer. On the other hand, if the reactivity of one of the two monomers is higher, a sequential IPN is likely to result. Obviously, between these two extreme cases, there are intermediate situations in which these molecular structures may coexist, depending on the reaction conditions and on the composition of the reactive mixture. A careful examination of the crosslinking mechanism is therefore in order to obtain some information on the molecular structure of such a complex network. Isothermal FTIR measurements are well suited for this purpose, since such a spectroscopic technique allows the real-time monitoring of the various reactive species present in the system.

In Figure 2 are reported the FTIR transmission spectra at various reaction times of a 100/30/100 parts per body weight of the TGDDM/DDS/BMI reactive mixture kept at 140°C.

In the 3700–2700 cm^{-1} range [Fig. 2(A)], as already noted, the primary amine shows two well-resolved absorptions at 3475 cm^{-1} [$\nu_{as}(NH_2)$] and at 3375 cm^{-1} [$\nu_{sym}(NH_2)$]. The peak at higher frequency is well suited for quantitation, provided that the interference of the component due to the BMI $\nu_{C=O}$ overtone at 3472 cm^{-1} is eliminated. This is accomplished by evaluating the initial intensity of the above peak by difference spectroscopy and subtracting this value, corrected for the sample thickness, to the integrated absorbance at 3475 cm^{-1}. It was checked that the initial reduced absorbance at 3472 cm^{-1} corresponded to the final value obtained when the primary amine groups were fully consumed and the 3475 cm^{-1} peak was no longer present.

The relative conversion of the primary amine groups, α_{NH2}, was evaluated in the usual way:

$$\alpha_{NH_2} = \frac{C_0 - C_t}{C_0} = 1 - \frac{C_t}{C_0} \tag{3}$$

and, for the Lambert–Beer's law:

$$\alpha_{NH_2} = 1 - \frac{\bar{A}_t^{3475}}{\bar{A}_0^{3475}} \tag{4}$$

where $\bar{A}_t^{3475}$ and $\bar{A}_0^{3475}$ are the integrated absorbances of the 3475 cm^{-1} peak at time t and 0, respectively, corrected for the sample thickness.

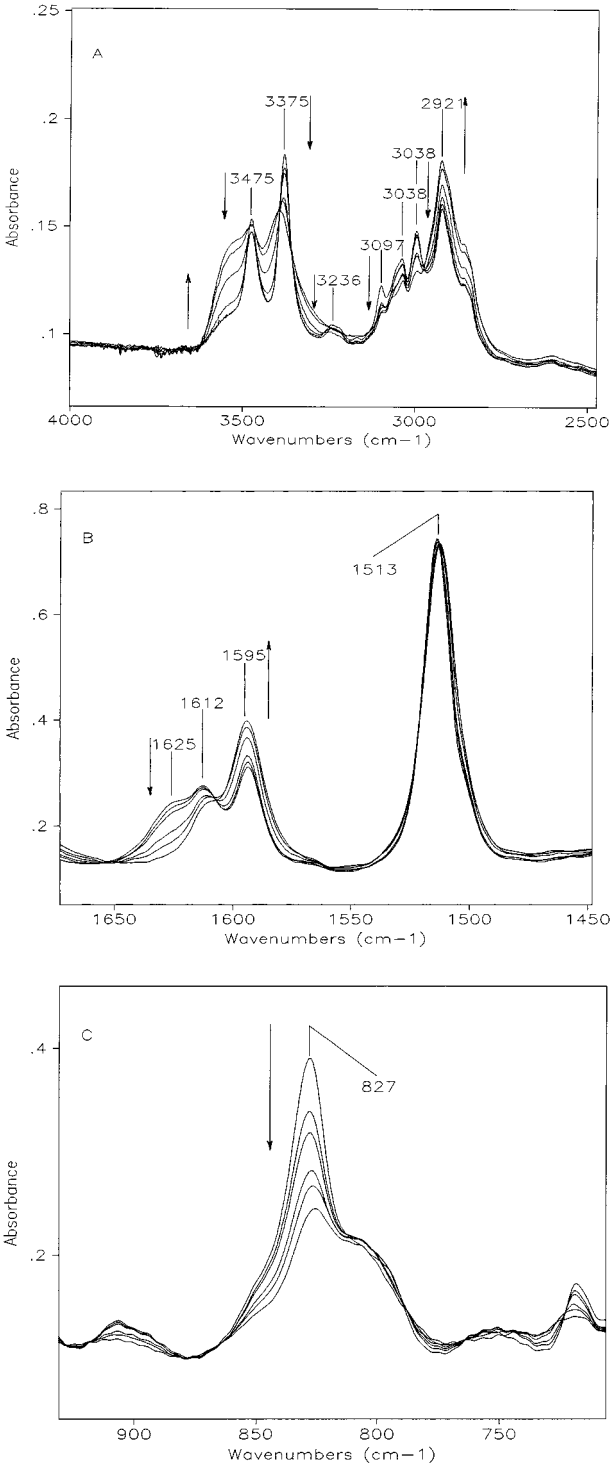

Figure 2 Transmission FTIR spectra of the TGDDM/DDS/BMI system at different reaction times for the process conducted at 140°C. The three figures display the frequency ranges used for quantitative analysis. The arrows' direction indicates absorbance increase or decrease of the relative peaks during the curing process.

The thickness correction was accomplished by dividing the analytical band by the invariant peak at 1513 cm^{-1} (a ring semicircle stretching mode of the diphenylmethane unit). Figure 2(B) evidences that the intensity of such an absorption hardly changes with the reaction time, thus indicating that the sample thickness remains approximately constant throughout the process.

The primary amine group gives rise to other two distinctive peaks: the first is a broad absorption located at 3236 cm^{-1} and is due to the first overtone of the δ (NH_2) fundamental at 1629 cm^{-1}. This latter band appears as a shoulder of the TGDDM aromatic absorption at 1612 cm^{-1}. Both of these peaks decrease gradually with time up to complete disappearance, thus confirming that the primary amine groups react to full conversion in the experimental conditions investigated.

The secondary amine group produces a ν(N—H) mode at 3395 cm^{-1} and an in-plane bending located at about 1600 cm^{-1}. Unfortunately both of these absorptions are completely overlapped, the former with the $\nu_{as}(NH_2)$ at 3375 cm^{-1} and the latter with the aromatic ring mode of DDS at 1595 cm^{-1}. Absolute quantitation is therefore unwarranted and only qualitative information on the concentration of secondary amines in the system has been derived. The hydroxyl groups produce the broad absorption between 3600 and 3200 cm^{-1} ($\nu_{O—H}$) which is observed to increase steadily with reaction time; the epoxy groups concentration was evaluated from the intensity of the well-resolved peak at 907 cm^{-1} (an oxirane ring stretching mode). Finally, with respect to the BMI unsaturation, Figure 2(A) shows the fast decrease of its characteristic absorption at 3097 cm^{-1}; in this case, however, incomplete conversion is attained by the end of the process. As already noted, because of severe overlapping, the 3097 cm^{-1} peak was considered unsuitable for quantitative purposes; instead, quantitation was accomplished by using the much better resolved absorption at 827 cm^{-1}, which is shown, at various reaction times, in Figure 2(C).

In Figure 3 are reported the relative conversions, α, as a function of the reaction time relative to the BMI double bonds (top curve) and to the epoxy groups (bottom curve). Both the curves show a similar shape and reach a plateau region close to 70% relative conversion; however, the initial conversion rate of BMI is considerably faster than that of the epoxy groups.

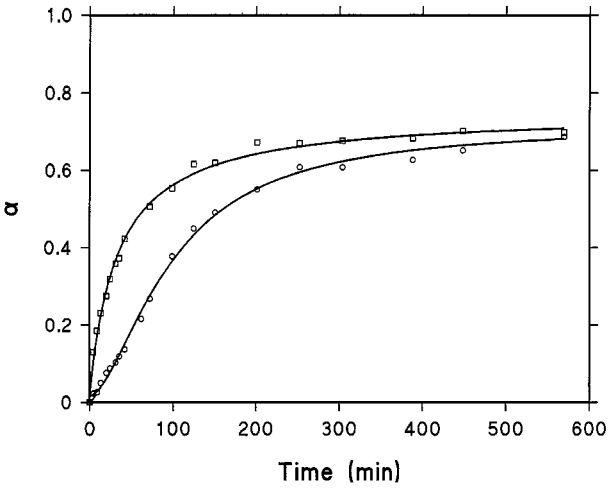

Figure 3 Relative conversion, α, of the epoxy groups (○) and the BMI double bonds (□) as a function of the reaction time in the system TGDDM/DDS/BMI.

Since the blend composition is nonstoichiometric, the concentration profiles of the various reactive species can be directly compared only if we consider the absolute conversion, $C_0—C_t$, which represents the number of reactive groups per unit mass consumed at time t. In terms of spectroscopic parameters, the absolute conversion is given by $C_0\alpha$ [i.e., $C_0(1 - \bar{A}_t/\bar{A}_0)$].

A plot of this type is reported in Figure 4(A) for the BMI double bonds (curve 2), the epoxy groups (curve 1), and the primary amine groups (curve 3). Figure 4(B) evidences the initial time period of the process (up to 125 min). Again, it is apparent that the BMI reacts much faster than the other two functionalities; in particular, the initial reaction rate of BMI, r_{BMI}, is 0.026 mol kg^{-1} min^{-1}, which is more than twice that of the epoxy groups, r_{EPO} = 0.011 mol kg^{-1} min^{-1} and about four times that of the primary amine groups, r_{NH2} = 0.0066 mol kg^{-1} min^{-1}.

Moreover, while the conversion curves relative to the epoxy and to the primary amine groups are highly linear in the first part (i.e., zero order), the BMI conversion curve displays a marked curvilinear shape. This suggests that the reaction mechanism of the BMI is different from that involving the epoxy and amine groups, whose concentration profiles show a close correlation, as if they were both involved in an independent reaction pathway to which the BMI groups do not participate.

Another interesting observation is that the curve relative to the NH_2 groups lies well below those of the BMI and the epoxy groups. This provides further evidence that BMI does not interact chemically with the primary amine through a Michael addition. In fact, if this reaction would prevail, the number of NH_2 groups consumed at any time would equal the absolute conversion of the BMI plus the number of epoxy groups reacted with the primary amines. Therefore, the NH_2 conversion curve would exceed both the BMI and the epoxy conversion curves, which is not what is experimentally observed.

Instead, as already noted, the experimental results seem to indicate that the BMI and the TGDDM/DDS pair follow two different and largely independent reaction pathways. The BMI

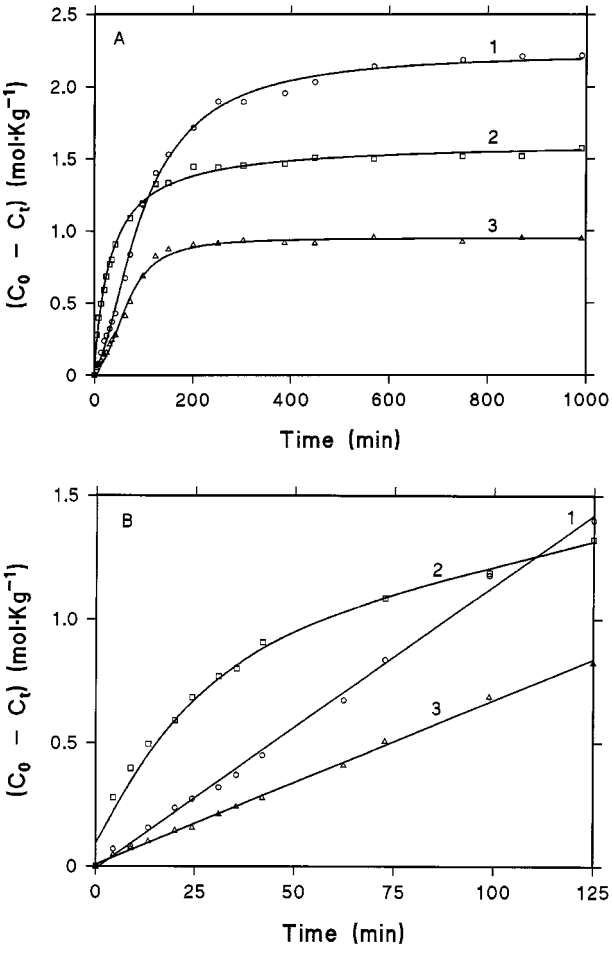

Figure 4 Absolute conversion as a function of the reaction time for the epoxy groups (curve 1), the BMI functionalities (curve 2), and the primary amine groups (curve 3) in the system TGDDM/DDS/BMI. (A) Whole time range. (B) Evidences the initial stage of the process.

crosslinks through a fast homopolymerization reaction, whereas the TGDDM/DDS gives rise to the condensation steps typical of this epoxy hardener pair, which have been previously mentioned. Thus, two chemically different networks are likely to build up simultaneously upon curing, with that due to the bismaleimide growing at a faster rate than that arising from the TGDDM/DDS. However, based on the dynamic-mechanical results to be discussed later, it emerges that, despite the different growing rates, the two networks exhibit a substantial degree of interpenetration.

The spectroscopic evidence suggests that, in this system, the homopolymerization of BMI is strongly favored over the Michael addition, contrary to what has been generally claimed in the literature. Furthermore, the reaction temperature of 140°C, is rather low for the neat BMI to be radically crosslinked at a substantial rate, as occurs in the system under investigation. A catalytic activity of TGDDM, which selectively accelerates the BMI homopolymerization could be the underlying reason for these effects. As a matter of fact, in a recent contribution,[20] it has been observed that, in epoxy compounds, at temperatures as low as 120°C, *N*-substituted maleimides polymerize to form maleimide oligomers with a degree of polymerization between 5 and 7. The reaction has been claimed to be anionically initiated by a zwitter-ion adduct formed by interaction between the oxirane rings and the BMI double bonds. The experimental results obtained with the TGDDM/DDS/BMI system seem to support the previous hypothesis; further investigations, through isolation of the reaction products in the early stages of the curing process, are currently underway to obtain further details on the reaction mechanism.

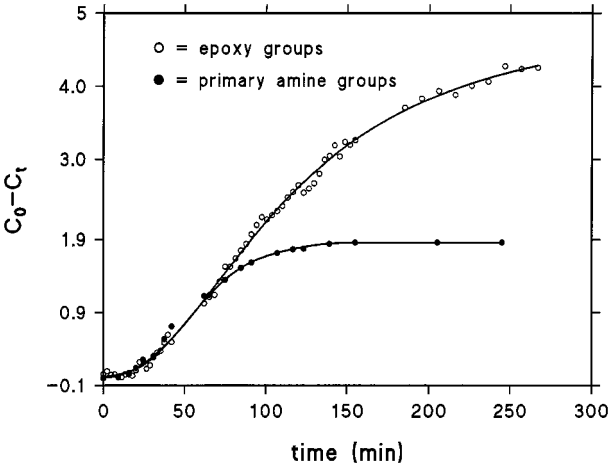

Figure 5 Absolute conversion as a function of the reaction time for the epoxy groups (○) and the primary amine groups (●) in the neat epoxy resin (TGDDM/DDS).

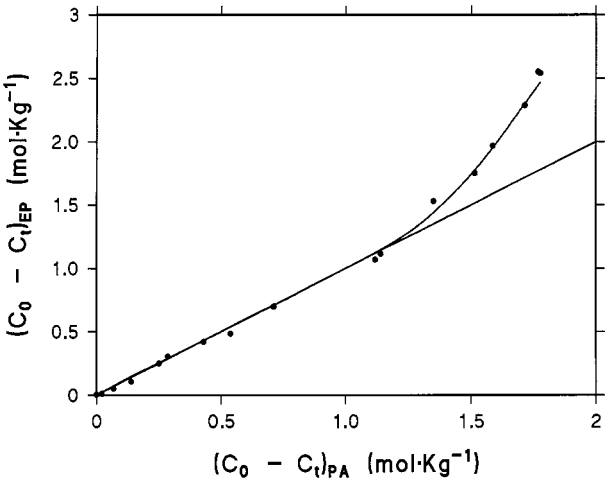

Figure 6 Absolute conversion of epoxy groups as a function of the absolute conversion of primary amine groups for the neat epoxy resin (TGDDM/DDS).

Turning the attention to the epoxy/hardener network, it is interesting to compare the kinetic behavior of the TGDDM/DDS pair in the 100/30/100 mixture with that of the neat TGDDM/DDS formulation, in the weight ratio of 100/30, cured at the same temperature (140°C). The absolute conversion as a function of time for the neat epoxy resin is reported in Figure 5, where the top curve refers to the epoxy groups, and the bottom curve is relative to the primary amine functionalities. It is observed that, in this case, the two curves coincide in the initial region. A further way of plotting the above data is on an epoxy-primary amine conversion-conversion diagram (Fig. 6); herein, the isoconversion line with slope = 1 represents a process in which each epoxy group reacts with a primary amine functionality (step 1 of the mechanism previously described). An up bending of the experimental data points would indicate the occurrence of steps 2 and/or 3 of the same mechanism. For the neat epoxy system at 140°C, the experimental points fall on the isoconversion line up to an amine conversion of 1.3 mol kg^{-1}, which corresponds to 70% of the initial content of primary amine. This clearly indicates that step 1 is the only one occurring in the system in the presence of primary amines. The other two

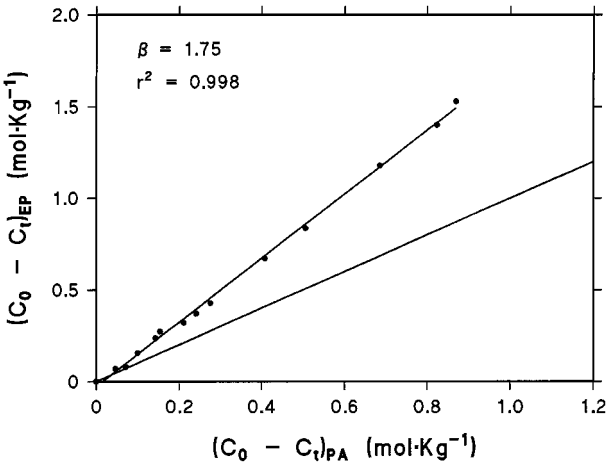

Figure 7 Absolute conversion of epoxy groups as a function of the absolute conversion of primary amine groups for the system TGDDM/DDS/BMI.

processes start to occur only when the concentration of NH_2 groups becomes negligible.

A completely different picture is found for the TGDDM/DDS/BMI system (see Fig. 7). In this case, data exhibit a linear behavior with a slope of 1.75, far exceeding that of the isoconversion line. Thus, for each amino group reacted, 1.75 epoxy groups are consumed, and this ratio remains constant up to the complete conversion of primary amines, which indicates the invariance of the overall reaction mechanism with the primary amine concentration. Evidently, contrary to what happens in the neat epoxy resin, in the TGDDM/DDS/BMI system, reaction steps 2 and 3 play a significant role even in the presence of primary amine groups, and the oxirane rings interact concurrently with both secondary amine and hydroxyl groups. This effect could be due to the presence of the fast growing BMI network that strongly hinders the molecular mobility of the reactants, forcing them to interact with their closest partners rather than being able to migrate to meet the more reactive functional groups, as occurs in the early stages of the curing process in the neat epoxy resin. In these conditions, intramolecular cyclization reactions, which have been demonstrated to occur even in the neat epoxy resin when cured with a rather low reactivity hardener as the DDS, are likely to be strongly favored:

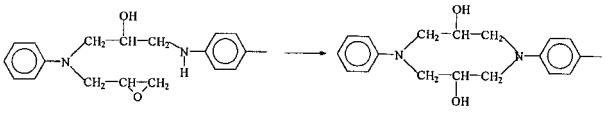

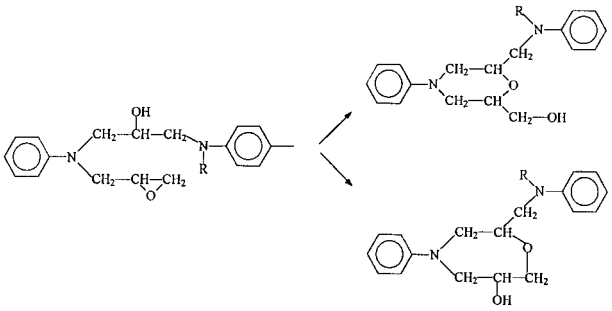

The formation of such small cyclic units has the effect of lowering the crosslinking density of the epoxy resin with respect to maximum attainable based on the reactants' functionality.

A further interesting difference that emerges by comparing the kinetic behavior of the neat epoxy resin with that of the TGDDM/DDS/BMI system concerns the shape of the conversion profiles. In fact, in the former case, we observe a sigmoidal shape that is not found in the latter case. The neat epoxy resin displays an initial induction period that is clearly related to the autocatalytic nature of the process, whereby a sudden increase of the reaction rate occurs as soon as a critical concentration of the groups that catalyze the reaction (the hydroxyl groups) is built up in the system. In the TGDDM/DDS/BMI system, this characteristic feature of the conversion profiles is absent: no induction period is observed and the reaction rate remains constant in the early stages of the process [see Fig. 4(B)]. Thus, in this case, the autocatalytic activity of the hydroxyl groups seems to be strongly hindered, possibly because of a dilution effect.

To summarize the results of the spectroscopic analysis, the experimental evidence discussed so far points to the formation of two distinct networks growing at different rates, the first formed by BMI homopolymerization, the second by the crosslinking of the TGDDM/DDS pair. The BMI network is likely to be rather defective, because the final conversion of the monomer does not exceed 70% and does not increase substantially upon postcuring. The molecular structure of the TGDDM/DDS network is considerably different from that of the neat epoxy/hardener system cured in the same experimental conditions. The presence of BMI, through a molecular mobility effect, enhances side reactions with secondary amines and hydroxyl groups, possibly favoring the formation of cyclic structures within the network.

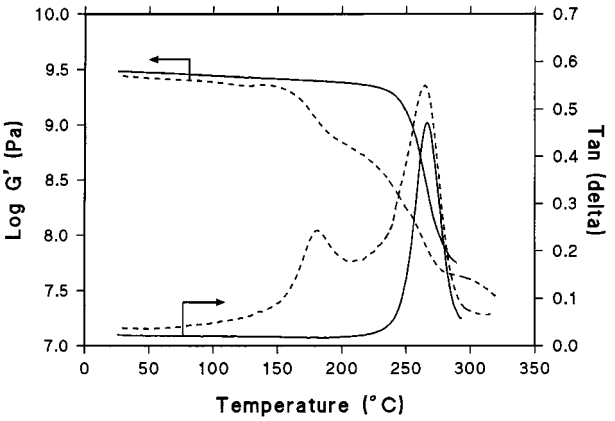

Figure 8 Dynamic-mechanical spectra of the neat epoxy resin. Solid lines refer to the dry sample. Dashed lines are relative to the sample after reaching the equilibrium water uptake.

No evidence of autocatalytic activity is found in the blend system.

Properties of the Dry Resins

The dynamic mechanical spectra of the neat TGDDM/DDS resin and of two typical blend compositions are reported in Figures 8–10. A single, symmetrical damping peak—analogous to that observed in the neat resin—is detected for all the investigated blend compositions. Its position shifts at higher temperatures as the BMI content in the blend increases. These observations can be interpreted by assuming that the BMI and the TGDDM/DDS networks formed upon curing possess a substantial degree of interpenetration and that the IPN system is molecularly homogeneous, at least up to the scale of the dynamic-mechanical test. In other words, the fact that the T_g of the investigated samples is well defined and only slightly broadened indicates that the phase domains are smaller than the size of the segments that are responsible for the primary molecular relaxation.[21]

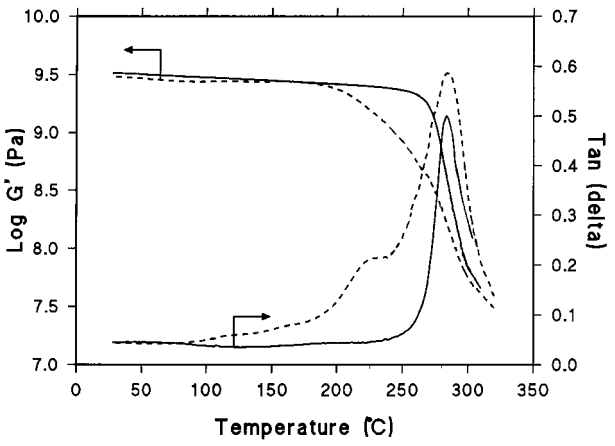

Figure 9 Dynamic-mechanical spectra of the TGDDM/DDS/BMI system of composition 100/30/50 by weight. Solid lines refer to the dry sample. Dashed lines are relative to the sample after reaching the equilibrium water uptake.

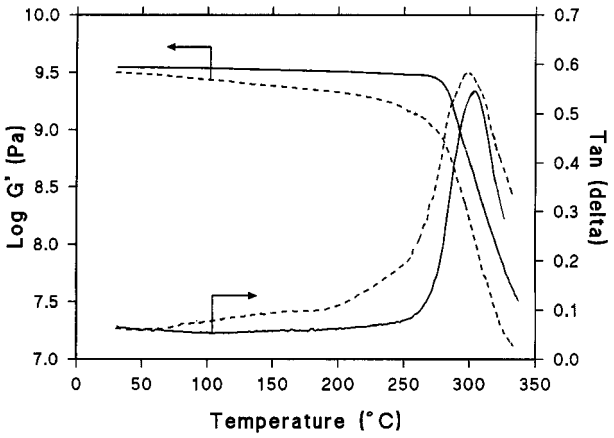

Figure 10 Dynamic-mechanical spectra of the TGDDM/DDS/BMI system of composition 100/30/100 by weight. Solid lines refer to the dry sample. Dashed lines are relative to the sample after reaching the equilibrium water uptake.

The glass transition temperatures, T_g, estimated as the temperature corresponding to the maximum of the tan δ peak, are reported in Figure 11 as a function of composition. The continuous line connecting the experimental data points represents the well-known Fox equation, which has been extensively used in calculating the T_g's of compatible IPNs and simultaneous interpenetrating networks (SINs).[22]:

$$\frac{1}{T_g} = \frac{w_1}{T_{g1}} + \frac{w_2}{T_{g2}} \qquad (5)$$

where T_{g1} and T_{g2} represent the glass transition temperatures of the TGDDM/DDS resin, and of a thermally cured BMI resin, respectively; w_1 and w_2 are their weight fractions, and T_g is the predicted value of glass transition temperature of the composite system. The T_{g2} value was not experimentally available, because extensive degradation of the BMI occurs concurrently with the onset

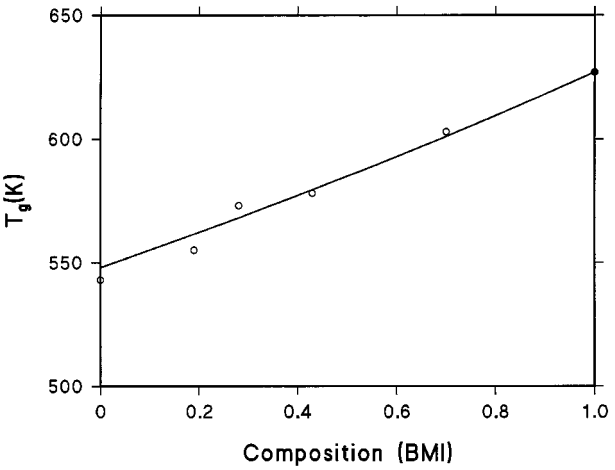

Figure 11 Glass transition temperatures, T_g, as a function of composition. Solid line represents the prediction of Fox's equation.

of large-scale molecular mobility. Therefore, the T_{g2} value was taken as an adjustable parameter to be determined by a least-squares refinement procedure. It was found that the experimental data points were well interpolated by the Fox equation and that the T_{g2} value determined in such a way (625 K) was reasonable for a cured BMI resin. Thus, a molecular structure consisting of two interpenetrated networks seems to be consistent with the observed dynamic mechanical behavior. We recall that, before the curing process, the TGDDM/DDS/BMI mixture is molecularly homogeneous. However, during curing, the molecules grow in size and the entropy contribution to the free energy of mixing decreases. As a consequence, phase separation tends to occur. The formation of mechanical interlocks, especially in a densely crosslinked network, may counter this tendency and essentially enhance phase homogeneity. It is mainly the occurrence of such high-density interlocks, not the formation of covalent bonds, that maintain phase homogeneity in the present system.[23]

Fracture measurements were performed on the investigated blend compositions, and experimental data were analyzed according to the linear elastic fracture mechanics approach. The critical stress intensity factor, K_c, and the critical strain energy release rate, G_c, are reported in Figure 12(A,B), as a function of the BMI content in the blend. Both the fracture parameters exhibit a gradual decrease up to a composition of about 30% body weight of BMI. Afterwards, the values of K_c and G_c remain almost unaffected. An opposite trend was observed for the flexural elastic modulus, E, whose value increases slightly with increasing the amount of BMI in the blend (see Fig. 13). The observed reduction of the fracture parameters may be ascribed to an increased rigidity of the network due to the presence of BMI, which renders the IPN system less able to undergo viscoelastic and plastic deformation processes. On the other hand, the enhancement of elastic modulus occurring when the BMI content in the blend increases reflects the higher stiffness of the BMI network with respect to that of the TGDDM/DDS matrix.

Properties of the Wet Resins

The kinetics of water absorption at 70°C for the neat epoxy resin and for two blend compositions

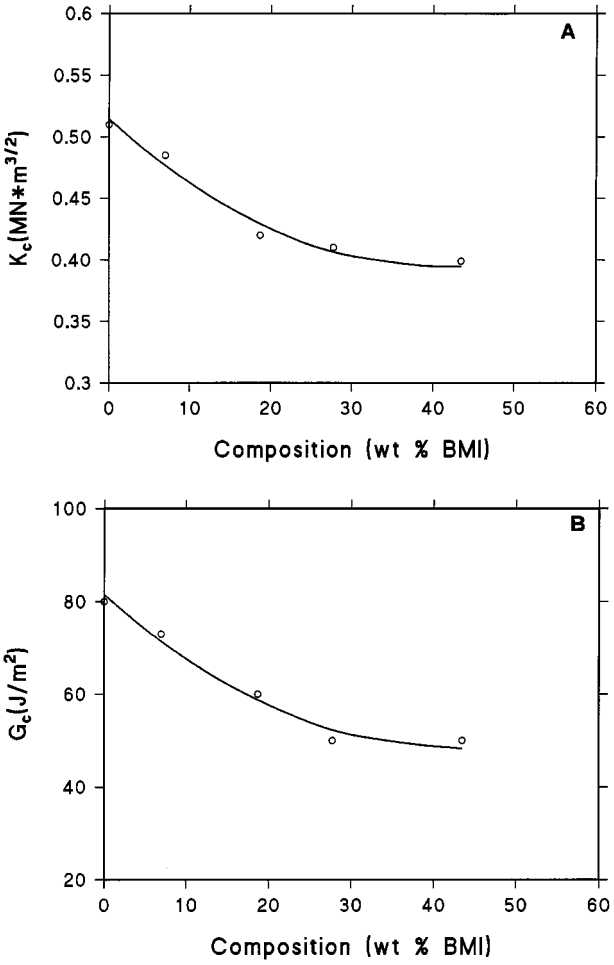

Figure 12 Critical stress intensity factor, K_c, (A) and the critical strain energy release rate, G_c (B) as a function of the composition of the reactive mixture.

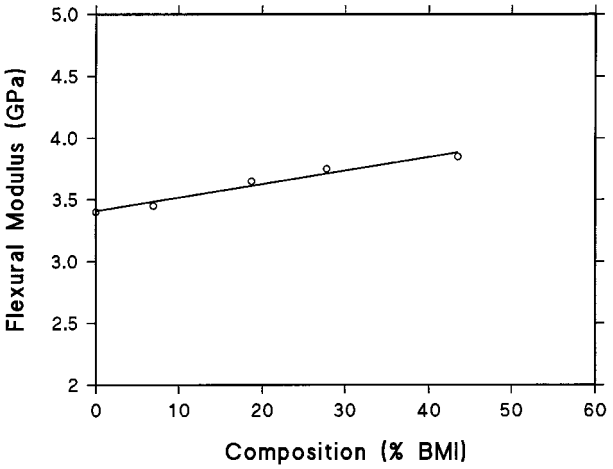

Figure 13 Elastic modulus, E, as a function of the composition of the reactive mixture.

containing 28 and 43.5 wt % of BMI, respectively, are collectively reported in Figure 14. Data were found to be linear when plotted against $\sqrt{t}/l$, thus indicating that all of the investigated materials behave according to the Fick's law of diffusion. The calculated diffusion coefficients were 2.14×10^{-6}, 2.67×10^{-6}, and 2.82×10^{-6} $mm^2\ s^{-1}$, respectively, whereas the equilibrium water content was found to be 5.2%, 4.9%, and 4.2%. It is apparent that inclusion of the BMI monomer into the formulation hardly affects the rate of water uptake, whereas a more pronounced effect is observed on the equilibrium value of absorbed water. However, the reduction of water uptake in the IPN system is lower than that expected when considering the negligible tendency of BMI to absorb moisture and the BMI concentration in the investigated specimens. It is likely that a more defective network is formed in the presence of BMI, which enhances the water absorption through purely physical mechanisms. Thus, the reduction of the network polarity is compensated for by a concurrent decrease of its perfection. As a matter of fact, such changes in the network topology should also affect the short-term absorption behavior (i.e., the diffusion coefficients). However, probably, the effect becomes too small to be readily detectable at 70°C. A deeper analysis of the diffusion behavior as a function of temperature is currently under way for a better understanding of these effects.

In Figures 8–10 are also compared the dynamic-mechanical spectra of the dry and water-saturated samples for the neat resin (Fig. 8) and for the two investigated compositions (Figs. 9 and 10).

The tan δ spectrum of the wet epoxy resin displays two well-resolved peaks, occurring at 181.5 and at 262°C. This behavior has already been reported in the literature,[24–27] but its interpretation is still controversial.

The low temperature peak is clearly due to the plasticizing effect of the absorbed water; however, for some authors,[22] heating of the sample during the dynamic-mechanical test causes its progressive drying. At about 210°C, the sample has lost almost completely the absorbed moisture and gives rise to a relaxation peak characteristic of the network in the dry state.

An alternative explanation was advanced by Mijovic and Tsay,[28] based on the assumption that, upon curing, the epoxy resin yields a heterogeneous structure with densely crosslinked, "nodular" regions, dispersed into a matrix having a lower crosslinking density. The diffusing water first saturates the looser epoxy network and then penetrates the nodular regions; it strongly plasticizes the internodular zone, but hardly affects the tightly crosslinked regions. Thus, the lower temperature relaxation peak represents the response of the plasticized internodular region, whereas the main tan δ peak is due to the noduli. Recently, however, Chateauminois and colleagues[29] showed that the splitting of the tan δ peak in water-saturated epoxy specimens has to be attributed to an enhanced drying of the specimens above the glass

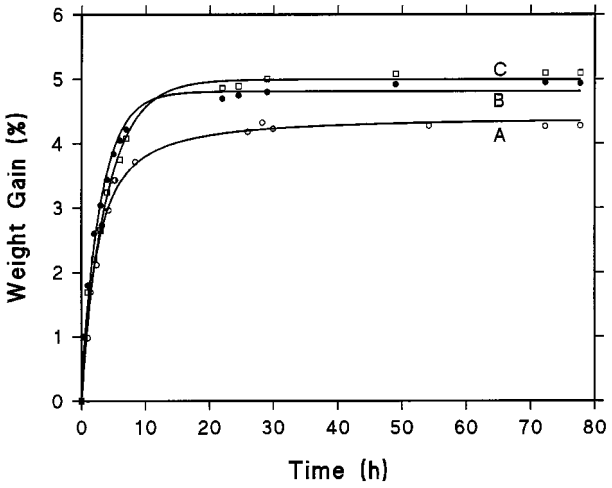

Figure 14 Sorption diagrams at 70°C for the neat epoxy resin (curve C), the 100/30/50 TGDDM/DDS/BMI blend (curve B), and the 100/30/100 TGDDM/DDS/BMI blend (curve A).

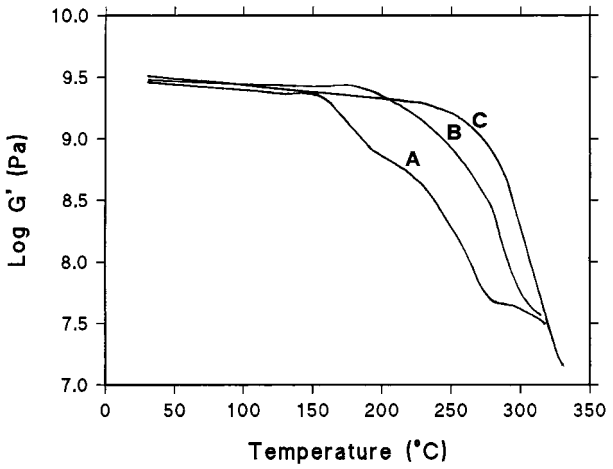

Figure 15 Storage modulus, G', as a function of temperature, for the water-saturated samples. (Curve A) TGDDM/DDS (100/30 body weight). (Curve B) TGDDM/DDS/BMI (100/30/50 body weight). (Curve C) TGDDM/DDS/BMI (100/30/100 body weight).

transition during the dynamic-mechanical measurement and that differential plasticization of the network at the aging temperature cannot be invoked.

In the presence of BMI, considerable differences are observed in the tan δ spectra of the wet samples: the low temperature component becomes broader and less pronounced, and shifts at higher temperature as the BMI content increases. For the blend containing 28% of BMI, the low temperature peak is still partially resolved from the main relaxation, whereas in the blend with 43.5% of BMI, it appears as a barely detectable shoulder on the left side of the principal component.

These effects can be interpreted assuming a faster drying of the BMI-containing specimens with respect to the plain epoxy resin in the experimental conditions of the dynamic-mechanical measurements. Thus, a larger amount of absorbed water is lost before reaching the first transition region and the plasticization efficiency is lowered (i.e., the low temperature peak is less pronounced and shifted toward higher temperatures).

In turn, the enhancement of the desorption rate by increasing the amount of BMI in the system might be due to the increasing amount of water absorbed through physical processes and not interacting at the molecular level with the network. This type of water possesses a higher degree of molecular mobility and is easier to be removed.

By comparing the storage modulus *versus* temperature curves of the wet samples (Fig. 15), it emerges an important aspect related to the application of such an IPN system. It is seen that the considerable drop of modulus due to the plasticizing effect of water, which, in the neat TGDDM/DDS resin, is observed about 100°C below the main relaxation, occurs at higher temperatures by increasing the BMI content in the system and tends to merge with the main relaxation. This effect could, in principle, reduce or eliminate one of the main drawbacks of the epoxy matrices (i.e., their decreasing stiffness and thermal stability in the wet state). It is clear that the extent of this effect depends on the experimental conditions and, in particular, on the heating rate and sample thickness. Nevertheless, it may safely be stated that, even if the amount of absorbed water at equilibrium is comparable, its plasticizing efficiency is gradually reduced as the amount of BMI in the system increases.

CONCLUSIONS

The kinetics and mechanism of the curing process of a TGDDM/DDS/BMI system was investigated in detail by FTIR. The results of the spectroscopic analysis were as following:

- Two different molecular networks are formed during the curing process: the first due to the BMI homopolymerization and the second to the cross-linking of the TGDDM/DDS pair.
- The BMI network grows at a higher rate than that formed by the TGDDM/DDS pair.
- The BMI network is likely to be rather defective, because the final conversion does not excede 70%. The presence of the BMI, through a molecular mobility effect, enhances the formation of small cyclic structures in the TGDDM/DDS network, thus lowering its crosslink density. No autocatalytic activity of the hydroxyl groups is detected in the blend system.

The dynamic-mechanical tests, performed on dry samples of blends of different compositions, indicated that, despite the different growing rates, the two networks possess a substantial degree of interpenetration. The fracture properties decreased slightly by increasing the BMI content in the system, whereas an opposite trend was observed for the flexural elastic modulus.

The water absorption measurements showed

that the presence of the BMI component slightly decreases the amount of absorbed water at equilibrium for measurements conducted at 70°C. No detectable differences were found in the apparent diffusion coefficients.

Finally, dynamic-mechanical measurements on wet samples demonstrated that, even if the equilibrium water uptake is comparable, the plasticizing efficiency of the absorbed water is gradually reduced as the amount of BMI in the system is increased.

REFERENCES

1. C. B. Bucknall and I. K. Partridge, *Polym. Eng. Sci.,* **26,** 54 (1986).
2. C. B. Bucknall and I. K. Partridge, *Polymer,* **24,** 339 (1983).
3. E. Martuscelli, P. Musto, G. Ragosta, and G. Scarinzi, in *Advanced Routes for Polymer Toughening,* E. Martuscelli, P. Musto, and G. Ragosta, Eds., Elsevier, Amsterdam, 1995, Chap. 1, p. 11.
4. S. Kunz-Douglass, B. W. R. Beaumont, and M. F. Ashby, *J. Mat. Sci.,* **15,** 1109 (1980).
5. A. J. Kinloch, in *Rubber Toughened Plastics,* C. K. Riew, Ed., *Advances in Chemistry Series,* **222,** 1989, Chap. 3., p. 67.
6. C. E. Browning, in *Advanced Thermoset Composites,* J. M. Margolis, Ed., Van Nostrand-Reinhold, New York, 1986, Chap. 1, p. 1.
7. J. G. Williams, in *Fracture Mechanics of Polymers, Ellis Horwood Series in Engineering Science,* 1984.
8. W. F. Brown and J. Srawley, *ASTM STP410,* American Society for Testing and Materials, Philadelphia, 1966, p. 13.
9. E. Plati and J. G. Williams, *Polym. Eng. Sci.,* **15,** 470 (1975).
10. D. O. Hummel, K. U. Heinen, H. Stenzeberger, and H. Siesler, *J. Appl. Polym. Sci.,* **18,** 2015 (1974).
11. C. Di Giulio, B. Gautier, and B. Jasse, *J. Appl. Polym. Sci.,* **29,** 1771 (1984).
12. S. F. Parker, S. M. Mason, and K. P. J. Williams, *Spectrochim. Acta,* **46A,** 121 (1996).
13. M. Abbate, E. Martuscelli, P. Musto, and G. Ragosta, in *J. Appl. Polym. Sci.,* **65,** 979 (1997).
14. B. Ellis, *Chemistry and Technology of Epoxy Resins,* Blackie Academic and Professional, London, 1993 (and references therein).
15. S. Varma, I. K. and D. S. Varma, *J. Polym. Sci., Polym. Chem. Ed.,* **22,** 1419 (1984).
16. A. V. Tugare and G. C. Martin, *J. Appl. Polym. Sci.,* **46,** 1125 (1992).
17. A. V. Tugare and G. C. Martin, *Polym. Eng. Sci.,* **33,** 614 (1993).
18. G. Pritchard and M. Swan, *Eur. Polym. J.,* **29,** 357 (1993).
19. K. F. Lin and J. C. Chen, *Polym. Eng. Sci.,* **36,** 211 (1996).
20. G. Lüders, E. Merker, and H. Raubach, *Die Ang. Makromol. Chem.,* **182,** 135 (1990).
21. O. Olabisi, L. M. Robeson, and M. T. Shaw, *Polymer-Polymer Miscibility,* Academic Press, London, 1979, Chaps. 2 and 3.
22. L. H. Sperling, *Interpenetrating Polymer Networks and Related Materials,* Plenum Press, New York, 1981.
23. E. M. Woo, L. B. Chen, and J. C. Seferis, *J. Mater. Sci.,* **22,** 3665 (1985).
24. J. Mijovic and F. K. Lin, *J. Appl. Polym. Sci.,* **30,** 2527 (1985).
25. J. P. Soulier, R. Berruet, A. Chateauminois, B. Chabert, and R. Gautier, *Polym. Com.,* **29,** 243 (1988).
26. J. M. Barton and D. C. L. Greenfield, *Br. Polym. J.,* **18,** 51 (1986).
27. B. De Neve and M. E. R. Shanadan, *Polymer,* **34,** 5099 (1993).
28. J. Mijovic and L. Tsay, *Polymer,* **22,** 902 (1981).
29. A. Chateauminois, B. Chabert, J. P. Soulier, and L. Vincent, *Polym. Comp.,* **16,** 288 (1995).